Published in final edited form as:
Nat Immunol. 2010 October ; 11(10): 912–919. doi:10.1038/ni.1933.

Caspase-12 controls West Nile virus infection via the viral RNA receptor RIG-I

Penghua Wang[1,4], **Alvaro Arjona**[1,4], **Yue Zhang**[1], **Hameeda Sultana**[1,3], **Jianfeng Dai**[1], **Long Yang**[1], **Philippe M LeBlanc**[2], **Karine Doiron**[2], **Maya Saleh**[2], and **Erol Fikrig**[1,3]

[1]Section of Infectious Diseases, Department of Internal Medicine, Yale University School of Medicine, New Haven, Connecticut, USA

[2]Department of Medicine, McGill University, Montreal, Quebec, Canada

[3]Howard Hughes Medical Institute, Chevy Chase, Maryland, USA

Abstract

Caspase-12 has been shown to negatively modulate inflammasome signaling during bacterial infection. Its function in viral immunity, however, has not been characterized. We now report an important role for caspase-12 in controlling viral infection via the pattern-recognition receptor RIG-I. After challenge with West Nile virus (WNV), caspase-12-deficient mice had greater mortality, higher viral burden and defective type I interferon response compared with those of challenged wild-type mice. *In vitro* studies of primary neurons and mouse embryonic fibroblasts showed that caspase-12 positively modulated the production of type I interferon by regulating E3 ubiquitin ligase TRIM25–mediated ubiquitination of RIG-I, a critical signaling event for the type I interferon response to WNV and other important viral pathogens.

Caspases are a family of aspartic acid–specific cysteine-dependent proteases mainly involved in apoptotic and inflammatory signaling pathways[1]. The inflammatory caspases, including caspase-1 (also known as interleukin-1β (IL-1β)-converting enzyme), caspase-4 (mouse caspase-11), caspase-5 and caspase-12 (A000495), are clustered on human chromosome 11q22.2–22.3 (mouse chromosome 9A1), which supports the idea that they originate from the same ancestral genes[2]. Caspase-1 and caspase-12 are two important components of the inflammasome signaling that senses bacteria, in which caspase-1 cleaves the precursor forms of IL-1β and IL-18 and caspase-12 counteracts caspase-1 activity[3–5]. Several studies have demonstrated that caspase-1 has an important role in viral immunity. As part of the NLRP3 (Nod-like receptor family, pyrin domain– containing 3) inflammasome, caspase-1 is required for immunity to influenza viruses[6–8]. Engagement of the viral RNA receptor RIG-I by certain viruses leads to activation of caspase-1-dependent inflammasome signaling by an NLRP3-independent mechanism[9]. The role of caspase-12 in

Correspondence should be addressed to M.S. (maya.saleh@mcgill.ca) or E.F. (erol.fikrig@yale.edu).
[4]These authors contributed equally to this work.

Accession codes. UCSD-Nature Signaling Gateway (http://www.signaling-gateway.org): A000495.

Note: Supplementary information is available on the Nature Immunology website.

AUTHOR CONTRIBUTIONS

P.W., A.A., M.S. and E.F. conceived hypotheses, analyzed data and prepared the manuscript; P.W. and A.A. designed and did experiments; Y.Z., H.S., J.D., L.Y., P.M.L. and K.D. aided in experiments; and all authors discussed the results and implications and commented on the manuscript at all stages. E.F. and M.S. contributed equally to this work.

COMPETING FINAINCLAL INTERESTS

The authors declare no competing financial interests.

viral immunity has not been addressed so far. Several nonsense mutations are present in the human gene encoding caspase-12, which result in a truncated protein with only the caspase-recruitment domain (CARD). In about 20% of people of African descent, a full-length variant is expressed, but it may be enzymatically inactive, as its catalytic Ser-His-Gly motif is altered to Ser-His-Ser. People with a full-length variant are hyporesponsive to endotoxins and are prone to severe sepsis[3]. Mouse caspase-12 is fully expressed with a mutation in the sequence encoding its catalytic domain that renders it an extremely inefficient enzyme. Although catalytically competent, caspase-12 is unable to cleave any known caspase proenzymes, apoptotic substrates, cytokine precursors or the endoplasmic reticulum protein targets of caspase-mediated proteolysis[10]. The only known substrate is itself, in which the cleavage occurs at the Ala-Thr-Ala-Asp319 motif both *in cis* and *in trans* and requires the caspase-12 catalytic activity[10]. This self-cleavage, however, is distinct from canonical caspase cleavage, as a pan-caspase inhibitor fails to block caspase-12 autoprocessing[11], which suggests that autoprocessing serves a purpose other than apoptosis. Caspase-12 has also been shown to bind to RIP2, the adaptor of the Nod pathogen pattern-recognition receptor, thus displacing the ubiquitin ligase TRAF6 from the signaling complex and dampening the production of antimicrobial peptides[11].

The putative role of caspase-12 in endoplasmic reticulum stress-induced apoptosis remains controversial. Early evidence showing caspase-12-mediated endoplasmic reticulum stress-induced apoptosis in response to amyloid toxicity[12] relied heavily on the cleavage of caspase-12, which may be a result of autoprocessing[10] or calpain cleavage[12,13] but not on caspase cascade processing. Moreover, the physiological relevance of caspase-12 cleavage remains incompletely understood, given the fact that the catalytic cysteine is dispensable for its effects on caspase-1 (ref. 4). Subsequent studies have shown that caspase-12 can be processed by the ubiquitin ligase TRAF2 (ref. 14) or caspase-7 (ref. 15). The cleaved products of caspase-12 can in turn directly or indirectly process caspase-9 and then caspase-3, which leads to cytochrome *c*–dependent or cytochrome *c*–independent apoptotic pathways[12,15–17]. These could be cell type– and/or stimulus-specific phenotypes, as caspase-12 is dispensable for apoptosis in mouse embryonic fibroblasts (MEFs)[4,18,19]. In addition, inflammatory stimuli can induce endoplasmic reticulum stress[20], which could explain the involvement of caspase-12 in endoplasmic reticulum stress-induced apoptosis.

Mosquito-borne flaviviruses of the family *Flaviviridae* are an increasing threat to human health. One of the life-threatening flaviviruses, West Nile virus (WNV), has spread rapidly throughout North America since 1999 and accounts for considerable morbidity and mortality in susceptible people. The innate immune response to WNV is mediated mainly by the Toll-like receptors TLR3 and TLR7 and the cytoplasmic RNA helicases RIG-I and Mda5 (refs. 21–23). *In vivo*, TLR3 signaling contributes to the innate immune response to WNV and limits viral dissemination in the periphery and the central nervous system (CNS)[24,25], whereas TLR7 helps clear viruses via IL-23-dependent immune cell infiltration and homing[26]. Systemically, RIG-I has a dominant role in initiating the innate immune response to WNV, whereas Mda5 amplifies and maintains it[27,28]. Under- or over-responsiveness to WNV can produce the same outcome—death—due to encephalitis by either uncontrolled viral replication or inflammation in the CNS. Thus, RIG-I signaling is finely regulated by host factors, ubiquitination[29,30], autophagy[31] or the RNA helicase LGP2 (refs. 32,33). The E3 ubiquitinase TRIM25 mediates ubiquitination of RIG-I, an essential step for its signaling and subsequent type I interferon response[29], whereas the E3 ubiquitin ligase RNF125 or autophagy sends RIG-I to proteasomes or lysosomes for degradation[30,31]. However, the regulation of RIG-I could be more complex than the present understanding would indicate. Here we investigate the role of caspase-12 in WNV infection and provide evidence that caspase-12 is required for an effective innate immune response to WNV via regulation of the ubiquitination of RIG-I.

RESULTS

Caspase-12 controls WNV infection *in vivo*

The NLRP3 inflammasome has been shown to be required for innate and adaptive immune responses to influenza viruses[6–8]. To determine whether NLRP3 inflammasome signaling is important for the host immune response to neurotropic WNV, we infected NLRP3-deficient (*Nlrp3*$^{-/-}$) mice with a sublethal dose of WNV. The overall survival in these mice was similar to that of the wild-type control mice (Supplementary Fig. 1), which suggested that the inflammasome does not have an important role in WNV pathogenesis. However, we found that mice deficient in caspase-12 (*Casp12*$^{-/-}$ mice), a negative regulator of inflammasome signaling[3–5], were significantly more susceptible to WNV-induced lethality than control mice were when challenged with either a low dose of virus (200 plaque-forming units (PFU)) via subcutaneous footpad inoculation or a high dose of virus (1,500 PFU) via intraperitoneal inoculation (Fig. 1a). In addition, *Casp12*$^{-/-}$ mice developed severe neurological symptoms, including limb weakness, tremor, ataxia and paresis (Supplementary Videos 1–3). To quantify the neurological deficit observed in *Casp12*$^{-/-}$ mice, we did footprint analyses at day 5 after infection via the intraperitoneal route. Compared with WNV-infected wild-type mice, *Casp12*$^{-/-}$ mice infected with WNV developed substantial alterations in the following gait parameters: step length (average distance of forward movement between alternate steps), step regularity (as measured by the sigma coefficient) and step uniformity (as measured by the alternation coefficient; Fig. 1b). These results are indicative of gait deterioration and cerebellar ataxia[34] and confirmed the WNV-induced neurological deficit in *Casp12*$^{-/-}$ mice. We then did virological analyses of peripheral and neural tissues. Viremia was significantly higher in *Casp12*$^{-/-}$ mice than in wild-type mice at day 4 after infection, as determined by quantitative real-time PCR analysis of WNV envelope (WNV-E) transcripts and plaque assay (Fig. 1c). We observed a similar trend in lung and spleen tissues. In line with the survival data and footprint analyses, the viral burden (as assessed by WNV-E and plaque assay) was greater in the CNS of *Casp12*$^{-/-}$ mice than that of wild-type mice at day 8 after infection by several orders of magnitude (Fig. 1d and Supplementary Fig. 2a). Lack of caspase-12 was also associated with more cell death in the CNS parenchyma (Fig. 1e and Supplementary Fig. 2b).

Caspase-12 facilitates the type I interferon response

Caspase-12 is known to dampen the immune response to bacterial infection by inhibiting the activity of caspase-1, which cleaves the cytokines IL-1β and IL-18 into their active forms[4]. Caspase-12 has also been shown to dampen mucosal immunity to bacterial infection independently of its effects on caspase-1 (ref. 11). The plasma concentrations of interferon-β (IFN-β) protein were significantly lower in WNV-infected *Casp12*$^{-/-}$ mice at days 2 and 4 after infection than in WNV-infected wild-type control mice (Fig. 2a). Both *Ifna* and *Ifnb* mRNA were also significantly lower at day 2 after infection in the absence of caspase-12, and the concentration of IFN-β protein was significantly lower than that of wild-type mice in the lung and liver, but not in the spleen, at day 4 after infection (Fig. 2b). Other inflammatory cytokines, including tumor necrosis factor (TNF) and IL-12p40, however, were not affected by the lack of caspase-12 at day 4 after infection in the peripheral tissues and serum (Supplementary Fig. 3). These data collectively suggest caspase-12 has a dominant role in the type I interferon response. We next examined type I interferon (mRNA and protein) and TNF (protein) in the CNS at day 8 after infection with a low dose of virus (200 PFU). There was modestly but significantly less type I interferon and TNF in *Casp12*$^{-/-}$ mice than in wild-type mice (Fig. 2c). This defective type I interferon response was more evident in mice infected with a high dose of virus, administered intraperitoneally or intracranially (Supplementary Fig. 4). To further confirm that neural tissues depend on caspase-12 for an adequate anti-WNV response, we isolated primary cortical neurons and

microglia from the brains of wild-type and *Casp12*$^{-/-}$ mice and quantified the viral load and type I interferon response after WNV challenge. *Casp12*$^{-/-}$ neurons had a higher viral load and less *Ifnb* mRNA than did wild-type neurons (Fig. 2d). However, caspase-12 was not required for the control of WNV infection or for the production of type I interferon in microglia, splenocytes or bone marrow–derived macrophages (Supplementary Fig. 5). These data are in line with the finding of an orders-of-magnitude higher viral burden in CNS tissues of *Casp12*$^{-/-}$ mice and suggest that caspase-12 shows certain cell specificity in its anti-WNV features. We then looked at differences in caspase-12 expression. Caspase-12 was induced more (~tenfold) as both protein and mRNA, coincidentally with the viral load (data not shown) in the encephalon (brain and cerebellum), at days 6–8 after infection than at day 4, when the virus starts to penetrate the CNS (Fig. 2e). In addition, the cleaved products of caspase-12 were evident as early as day 6 after infection (Fig. 2e). RIG-I, one of the main host pattern-recognition receptors for WNV, was also induced substantially by WNV in the CNS, whereas TRIM25 remained unchanged during the course of infection (Fig. 2e). We noted that after infection with WNV, several tissues had much higher expression of *Casp12* mRNA than did peripheral blood cells (Fig. 2f). This may partially explain why caspase-12 is not important for the control of WNV infection in some of the cells of the immune response tested.

To further evaluate our *in vivo* findings, we isolated MEFs from embryos at day 14 and examined their response to WNV infection. Consistent with our *in vivo* observations, caspase-12 expression was induced by WNV infection, and lack of caspase-12 in MEFs significantly augmented WNV infection by sixfold as early as 12 h after infection (Fig. 3a). WNV-E transcripts (as measured by quantitative PCR), WNV-E protein (as assessed by immunofluorescence microscopy) and the nonstructural viral proteins NS3 and NS2b (as assessed by immunoblot analysis) were much greater in abundance in *Casp12*$^{-/-}$ MEFs than in wild-type cells (Fig. 3a–c). The endoplasmic reticulum stress response is an innate response to microbial insult, and some reports indicate that it may be caspase-12 dependent[12]. Our results, however, showed that protein expression of the endoplasmic reticulum stress markers GRP94 and PDI was not lower in *Casp12*$^{-/-}$ MEFs (Fig. 3c). Published studies have also indicated involvement of caspase-12 in endoplasmic reticulum stress-induced caspase-3-mediated apoptosis[12,15–17]. We found that caspase-3 enzymatic activity in *Casp12*$^{-/-}$ MEFs was the same as that of wild-type cells (Supplementary Fig. 6a). To determine if the catalytic domain of caspase-12 is important for its antiviral function, we overexpressed rat wild-type caspase-12 and a catalytically incompetent mutant of caspase-12 (C299A)[10] in MEFs, followed by infection with WNV. Overexpression of either the wild-type or mutant caspase-12 inhibited WNV infection substantially to a similar extent at 24 h after infection (Supplementary Fig. 6b). As our *in vivo* results indicated that lack of caspase-12 affected production of type I interferon the most, we investigated whether this was also true for MEFs. We found that the production of IFN-α and IFN-β was much lower in *Casp12*$^{-/-}$ MEFs, as both mRNA and protein (Fig. 3d and Supplementary Fig. 7a,b). Consequently, less type I interferon in *Casp12*$^{-/-}$ MEFs also led to attenuation of the downstream antiviral gene *Isg15* (Supplementary Fig. 7c). The main WNV RNA–sensing molecule RIG-I (ref. 27) was also downregulated (as protein and mRNA) in *Casp12*$^{-/-}$ cells as early as 12 h after infection, even though the WNV NS3 and NS2b proteins were greater in abundance (Fig. 3e and Supplementary Fig. 7d). However, after infection with WNV, lack of caspase-12 did not substantially affect the mRNA for Mda5, another viral pattern-recognition receptor, or MAVS (Cardif, VISA or IPS-I), the mitochondrial adaptor for RIG-I and Mda5 (Supplementary Fig. 7e,f). These results are in line with published reports suggesting that RIG-I has an important anti-WNV role in MEFs[27] and collectively indicate that caspase-12 mediates its interferon-promoting effect via RIG-I. To confirm that caspase-12 specifically targets RIG-I signaling, we tested infection of *Casp12*$^{-/-}$ MEFs with Sendai virus (SeV), which is sensed specifically by RIG-I, and encephalomyocarditis virus

(EMCV), which is recognized mainly by Mda5 (ref. 35). Knockout cells were more permissive to SeV than were wild-type cells, as assessed by the viral NP3 mRNA, and produced less IFN-β (protein and mRNA) than wild-type cells did (Fig. 3f). The concentrations of the protein products of selected interferon-stimulating genes (ISG proteins), including IRF7, ISG15, RIG-I and STAT1, and nuclear interferon-regulatory factor 3 protein were consistently lower in *Casp12*$^{-/-}$ MEFs than in wild-type MEFs (Fig. 3g). However, caspase-12 was not important for the type I interferon response to EMCV infection (Supplementary Fig. 8), which supports the idea of caspase-12-specific regulation of RIG-I.

Signaling through IFN-α and IFN-β receptors serves a critical antiviral role by inducing many antiviral genes and amplifying the interferon response. We next examined whether the type I interferon signaling pathway is functional in *Casp12*$^{-/-}$ cells. We pretreated MEFs with recombinant IFN-β and then assessed their infection with WNV. Our results indicated that pretreatment with recombinant IFN-β was able to lower the WNV burden (as assessed by mRNA) in *Casp12*$^{-/-}$ cells to the burden in untreated wild-type MEFs (Fig. 4a), which emphasizes the relevant role of type I interferon in the control of WNV replication. Exogenous IFN-β treatment was also able to fully restore the expression of RIG-I and ISG15 in *Casp12*$^{-/-}$ MEFs to that of untreated wild-type MEFs (Fig. 4b–c), but it was unable to restore endogenous *Ifnb* mRNA expression (Fig. 4d). These results show that *Casp12*$^{-/-}$ MEFs have intact IFN-β receptor signaling and faulty RIG-I signaling. That proposal was further strengthened by experiments with IFN-β treatment alone, in which all the ISG proteins we assessed were induced equally well in *Casp12*$^{-/-}$ MEFs and wild-type MEFs (Fig. 4e).

Caspase-12 regulates RIG-I signaling via TRIM25

The physical interaction between RIG-I and caspase-12 suggested a potentially functional interaction. The two CARDs of RIG-I are responsible for protein-protein interactions. However, these domains are masked by a repression domain in resting cells[36]. Thus, we used only the two CARDs to assess the RIG-I–caspase-12 interaction in MEFs. A construct of the two CARDs conjugated to glutathione S-transferase (GST-2CARDs) was able to precipitate caspase-12 and also V5-tagged TRIM25, a positive control that has been demonstrated to bind the two CARDs of RIG-I (ref. 29; Fig. 5a). Notably, purified recombinant caspase-12 was able to directly bind to GST-2CARDs but not to GST-TRIM25 (Fig. 5b). We then did immunofluorescence microscopy to see if caspase-12 and RIG-I localized together in WNV-infected MEFs and primary cortical neurons. Many caspase-12–stained structures localized together with RIG-I (Fig. 5c).

TRIM25-mediated ubiquitination of RIG-I has been shown to be essential for RIG-I-mediated antiviral signaling[29]. To determine whether caspase-12 is involved in this process, we introduced a RIG-I expression construct into wild-type and *Casp12*$^{-/-}$ MEFs and affinity purified the ubiquitinated proteins. Total protein ubiquitination was greater in *Casp12*$^{-/-}$ cells, probably due to their higher viral load (Fig. 6a). These ubiquitinated proteins were mainly cellular proteins, as we failed to detect any viral proteins (data not shown). Although TRIM25 protein expression was similar in whole-cell extracts of wild-type and *Casp12*$^{-/-}$ MEFs, ubiquitinated RIG-I was much lower in abundance in *Casp12*$^{-/-}$ cells (Fig. 6b). To further confirm that finding, we introduced a Flag-tagged RIG-I expression plasmid into MEFs, followed by infection for 24 h with WNV. Flag-tagged RIG-I was immunoprecipitated with an antibody to Flag. There was less ubiquitinated RIG-I in *Casp12*$^{-/-}$ cells than in wild-type cells (Fig. 6c). This defect in RIG-I ubiquitination seen in *Casp12*$^{-/-}$ MEFs had physiological effect on the type I interferon response. Overexpression of RIG-I and TRIM25 resulted in three- to fourfold more *Ifna* and *Ifnb* transcripts at a very early stage of WNV infection in wild-type cells, whereas we did not observe this effect in

Casp12$^{-/-}$ cells (Fig. 6d). In addition, the expression of RIG-I and TRIM25 in *Casp12*$^{-/-}$ cells was similar to that in wild-type cells (data not shown). The two CARDs of RIG-I are subject to robust TRIM25-mediated ubiquitination[29]. Consistent with that, CARD ubiquitination was enhanced in wild-type cells overexpressing wild-type TRIM25 but not in those overexpressing TRIM25 lacking the RING-finger domain. However, TRIM25-mediated ubiquitination of the CARDs in *Casp12*$^{-/-}$ cells was ~35% as much as that in wild-type cells (Fig. 6e). It has been also shown that the CARDs of RIG-I are able to induce type I interferon autonomously[29]. We next determined if this signaling requires caspase-12. Overexpression of GST-2CARDs was able to upregulate *Ifnb* eightfold in wild-type cells but only twofold in *Casp12*$^{-/-}$ cells (Fig. 6f).

DISCUSSION

The role of caspase-12 as an attenuator of the immune response to bacterial infection has been well documented[3,4,11], but its function in viral infection has not been examined directly. Here we have provided evidence demonstrating that caspase-12 was required for an effective innate immune response to WNV infection through its action on the viral pattern-recognition receptor RIG-I. We found that WNV-infected *Casp12*$^{-/-}$ mice had lower survival, exacerbated neurological symptoms and a greater viral burden. Instead of acting as an attenuator, caspase-12, through the regulation of TRIM25-mediated ubiquitination of RIG-I, was required for the type I interferon response to WNV. However, the literature remains controversial about the role of caspase-12 in virus-induced apoptosis[18,19,37–40]. The *in vitro* results that we have reported here also support the idea that caspase-12 is neither essential for virus-induced endoplasmic reticulum stress nor essential for apoptosis.

Neuroinvasion by WNV causes an acute, sometimes fatal, encephalomyelitis that results from neuronal death mainly via degenerative necrosis or apoptosis[41,42]. Uncontrolled WNV replication in the CNS of *Casp12*$^{-/-}$ mice contributed to their higher mortality rate than that of wild-type mice. It has been proposed that the long-term neurological sequelae of infection with WNV, such as defective motor function, limb weakness and paralysis, probably represent a considerable source of morbidity in patients after their recovery from acute illness[43]. Because of their unique neurological phenotype, which partially resembles the clinical features of WNV encephalitis, WNV-infected *Casp12*$^{-/-}$ mice may be a valid model for testing candidate therapeutics for the treatment of the neurological symptoms of viral encephalitides.

How does caspase-12 limit WNV replication? Our results showed that caspase-12 was required for an effective antiviral immune response, especially for the production of type I interferons. Caspase-12 was dispensable for IFN-β receptor signaling, as *Casp12*$^{-/-}$ cells responded to recombinant IFN-β as well as wild-type cells did. Instead, caspase-12 was crucial for the production of type I interferon in response to WNV infection. We did not observe any difference in proinflammatory cytokines such as TNF and IL-12 in the periphery. This could have been due to the inhibitory function of caspase-12 on IL-1β maturation, which might contribute to the expression of pro-inflammatory cytokines[4,11]. Our results showed that the consequences of an attenuated innate immune response in WNV replication were greater in the CNS than in the periphery. This may have been due to the immune-privileged nature of the CNS, as cellular immunity can be more readily mobilized to help control dissemination of virus in the periphery. Moreover, caspase-12 was considerably induced in the CNS after WNV infection, and CNS tissues had much higher expression of caspase-12 (~50- to 100-fold) than peripheral blood cells at the peak of viral infection. All these considerations might explain why the antiviral function of caspase-12 is particularly important in the CNS. *In vitro*, we observed the importance of caspase-12 in limiting viral replication in MEFs as well as in primary neurons but not in splenocytes,

macrophages or microglia. This cell type–specific phenomenon was probably due to differences in the expression of caspase-12; that is, MEFs and neurons expressed more caspase-12 protein than did macrophages or splenocytes (200- to 300-fold and five- to tenfold more, respectively) with or without WNV infection (data not shown). Another factor might be the degree of dependence of the type I interferon response on RIG-I and presence of redundant pattern-recognition receptor signaling pathways in different cell types.

Our *in vitro* data further demonstrated that caspase-12 regulated the anti-WNV immune response at the level of viral RNA sensors. First, type I interferon expression reached its peak much later (12 h) in *Casp12*$^{-/-}$ cells than in wild-type cells but was still not completely abolished in these cells. Moreover, caspase-12 was important for the type I interferon response to SeV (a mainly RIG-I-activating virus) but not the response to EMCV (a mainly Mda5-activating virus). Of note, a published study has shown that RIG-I is critical for initiating and maintaining anti-WNV immune responses, whereas Mda5 has only a maintenance role. Loss of both RIG-I and Mda5 completely abolishes the innate antiviral response to WNV in MEFs[27]. Therefore, the results mentioned above indicate that caspase-12 specifically regulates RIG-I signaling. Second, ubiquitination of RIG-I, the main sensor in MEFs and *in vivo* for WNV double-stranded RNA, was compromised in *Casp12*$^{-/-}$ cells. RIG-I ubiquitination by different E3 ligases can lead to different consequences[29,30]. Our results also showed that caspase-12 was important for TRIM25-mediated ubiquitination of RIG-I and its downstream type I interferon response. Overexpression of TRIM25 enhanced IFN-β production in wild-type cells but not in *Casp12*$^{-/-}$ cells, which indicates that caspase-12 regulates TRIM25 activity. Caspase-12 potentially helps recruit RIG-I to TRIM25. Indeed, caspase-2 and caspase-8 are able to directly or indirectly recruit the ubiquitin ligase TRAF2 and RIP1 to activate transcription factor NF-κB signaling[1]. Caspase-1 can directly interact with RIP2 through their CARDs in the TLR- or T cell antigen receptor–mediated NF-κB signaling pathway[44]. It has also been suggested that the prodomains of caspase-8 and caspase-10 act downstream of RIG-I or Mda5 to activate NF-κB signaling[45]. In agreement with our observations, the nonapoptotic function of these caspases does not always require their enzymatic activity[1]. However, caspase-12 has been shown to serve as a dominant negative binder of caspase-1 to inhibit IL-1β maturation and a negative interactor of RIP2 to displace TRAF6 (refs. 4,11). The varying roles for caspases depending on the disease, tissue and infectious agent are not unexpected. A good example of this is caspase-1, which is critical for IL-1β maturation after bacterial infection but downregulates antiviral RIG-I signaling by promoting its secretion from cells[46]. The inhibitory function of caspase-12 on caspase-1-mediated IL-1β maturation could be of considerable physiological importance during the course of viral infection. This dual functionality of caspase-12 could maximize host antiviral effects by limiting the production of mature IL-1β, which would inhibit the IFN-β response[47] and in the meantime minimize the immunopathological consequences of IL-1β.

Estrogen represses caspase-12 expression, which may help females fight bacterial infection[48]. Notably, estrogen has also been shown to downregulate the antiviral response to RNA viruses in dendritic cells by suppressing the production of type I interferon[49]. It is plausible that estrogen affects the production of type I interferon in response to viral infection partly because of its effect on caspase-12 expression. The putative consequences of variations in the concentration of estrogen (both physiological and pathological) on susceptibility to flavivirus infection warrant further investigation. However, full-length caspase-12 is expressed in only ~20% of people of African descent and is associated with bacterial sepsis that is more prevalent in African Americans than other groups[3]. It is possible that sepsis could be involved in the selection of truncated caspase-12 over full-length caspase-12. However, this selection, like malaria resistance and sickle cell disease, could pose a disadvantage in fighting viral infections, including infection with WNV. Thus, it

would be also useful to investigate whether full-length caspase-12 is associated with resistance to neurotropic viral infection or whether the short form of human caspase-12 is also able to modulate the antiviral response.

In summary, we have reported here an antiviral role for caspase-12 both *in vivo* and *in vitro*. We found that caspase-12 was required for an effective interferon response through the regulation of TRIM25-mediated ubiquitination of RIG-I. Our study offers new insight into the complex regulatory machinery for antiviral signaling pathways that could be exploited for therapeutic purposes.

ONLINE METHODS

Animals and infection

All animal experimental protocols were approved by the Institutional Animal Care and Use Committee of Yale University. All animal infection experiments were done in a Biosafety Level 3 animal facility according to the regulations of Yale University. Age- and sex-matched mice (8- to 12-week-old C57BL/6 and *Casp12*$^{-/-}$ mice) were infected with WNV at a sublethal dose of 1,500 PFU intraperitoneally, 100 PFU intracranially or 200 PFU subcutaneously and were maintained in the Biosafety Level 3 animal facility. *Casp12*$^{-/-}$ mice have been described[4]. WNV (CT-2741) was isolated from naturally infected wild birds and was passaged *in vitro* once in Vero cells (African green monkey kidney cells). SeV (Cantell strain; VR-907) and EMCV (VR-129B) were from American Type Culture Collection. Animals were perfused thoroughly after anesthetization when tissues were needed for analysis. MEFs were prepared as described[4]. Primary neurons and microglia were isolated from embryos at embryonic days 16–18 and newborns at postnatal days 1–3, respectively, by standard methods.

Chemicals and reagents

Rabbit anti-GRP94 (2104), anti-PDI (2446), anti-ISG15 (2743), anti-STAT1 (9172), anti-RIG-I (3743), anti-Flag–horseradish peroxidase (2044) and anti-β-actin (4968) were from Cell Signaling Technology; rabbit anti-IRF7 (SC-9083) was from Santa Cruz Biotechnology; goat anti-GST (27-4577-01) was from GE Healthcare; rabbit anti-TRIM25 (12573-1-AP) was from Proteintech Group; and anti–V5-tagged horseradish peroxidase (R961-25) was from Invitrogen. Goat antibody to NS2b and NS3 (AF2907), rabbit anti-caspase-12 (AF1456), and the IFN-β ELISA kit and recombinant IFN-β (41410 and 12400) were from R&D Systems. The Neocleofector kit was from Lonza and the polyubiquitinated protein enrichment kit was from EMD Biosciences. Anti-WNV-E (immunoglobulin G) conjugated to TRITC (tetramethylrhodamine isothiocyanate) was a gift from L2 Diagnostics.

Footprint analysis

A published procedure was used for footprint analysis[50]. Hind feet were coated with nontoxic ink and mice were allowed to walk on white paper. The footprint pattern generated was assigned scores for three parameters: step length (average distance of forward movement between alternate steps), defined as the distance of travel through the tunnel divided by the number of steps; sigma (regularity of step length), defined as the standard variation of all right-right and left-left step distance (higher sigma indicates less regular steps); and alternation coefficient (uniformity of step alternation), calculated as the mean of the absolute value of 0.5 minus the ratio of right-left distance to right-right step distance for every left-right step pair (high alternation score indicates lack of uniformity). These parameters have been used successfully in mouse models of cerebellar ataxia[34].

Construction of expression plasmids and transfection

The plasmids pcDNA 3.1-Casp12 and pcDNA 3.1-Casp12C299A have been reported[4]. The human RIG-I–expressing plasmid pUNO-RIG-I is a product of InvivoGen. For construction of the Myc-tagged mouse TRIM25–expressing plasmid, mouse MEF cDNA was amplified by PCR with gene-specific primers and the PCR products were then inserted into pCMV-Myc (Clontech). For recombinant GST– caspase-12, GST-TRIM25 (mouse) or GST-2CARD (mouse), pcDNA 3.1-Casp12 or mouse cDNA was amplified by PCR and the DNA fragments were inserted into pGEX-6p-2 (GE Healthcare). The caspase-12 PCR product was inserted into the pEGFP-C1 (Clontech) vector to make the GFP– caspase-12 plasmid. The expression plasmids pEGB (GST), pEGB-RIG-I2 CARDs (GST-2CARDs; human), human Flag-RIG-I and 2CARDs, human V5-tagged TRIM25 and V5-TRIM25 lacking RING[29] were gifts from J.U. Jung. For transfection, an electroporation method was used (Lonza).

Biochemical assays

For enrichment of ubiquitinated proteins (GST precipitation), cells were treated for 0.5 h with 10 μM MG132 (proteasome inhibitor), then lysed. Purification of ubiquitinated proteins essentially followed the manufacturer's product manual (EMD Biosciences). Immunoblot analysis was done by standard procedures except that in some cases SuperSignal substrate (ThermoFisher Scientific) was used. The caspase-3 colorimetric assay was done essentially according to the manufacturer's manual (BioVision), as was the IFN-β ELISA (R&D Systems). Serum TNF and IL-12p40 were quantified with Bio-Plex bead-based assays (Bio-Rad).

Flag and GST-precipitation assays

MEFs were cultured in MEM supplemented with 10% (vol/vol) FBS and were transiently transfected with Flag-tagged or GST-expressing plasmids with an MEF-specific electroporation reagent (Lonza). At 20 h after transfection, MEFs were lysed in lysis buffer (50 mM Tris-HCl, pH 7.4, 0.5% (vol/vol) Nonidet P-40, 2 mM EDTA and 150 mM NaCl, with complete protease inhibitors). Lysates were cleared by centrifugation and then were incubated for 2 h at 4 °C with M2 agarose beads (for Flag proteins; Sigma-Aldrich) or glutathione (GSH) agarose beads (for GST proteins; GE Healthcare), followed by five washes of the beads with lysis buffer. Immunoprecipitates on M2 beads were eluted with Flag peptides (Sigma-Aldrich); GST precipitates were eluted with 2× SDS-PAGE sample buffer.

Immunofluorescence microscopy and TUNEL staining

Mouse tissues were fixed in 4% (vol/vol) paraformaldehyde and were sectioned in paraffin. Immunofluorescence staining was done according to published standard protocols[26]. For TUNEL (terminal deoxynucleotidyl transferase-mediated dUTP nick end labeling), samples were stained with a kit from Promega. With this procedure, apoptotic nuclei are stained dark brown. Images were acquired with a Zeiss fluorescence microscope. Specimens were assigned scores of 0–3 (where 3 represents the greatest number of apoptotic cells) by a double-blinded process.

Quantitative real-time PCR and plaque-forming assay

Quantitative PCR was done with gene-specific primers and 6FAM-TAMRA (6-carboxyfluorescein–*N,N,N′,N′*-tetramethyl-6-carboxyrhodamine) probes[26] or inventoried gene expression kits from Applied Biosystems (6FAM-MGB (6-carboxyfluorescein–minor groove binder) probes). Plaque-forming assays of tissues or plasma were done as described[26]. Plasma (100 μl) diluted 10- to 100-fold with sterile PBS or 30–100 μg (total

protein) of tissue lysates triturated in sterile PBS was applied to confluent Vero cells. Plaques were visualized with Neutral Red (Sigma-Aldrich) after 3 d of infection.

Graphing and statistics

Prism 4 software (GraphPad Software) was used for survival curves, charts and statistical analyses. The significance of results was analyzed by an unpaired two-tailed Student's *t*-test or nonparametric Mann-Whitney test, with a cutoff *P* value of 0.05.

Supplementary Material

Refer to Web version on PubMed Central for supplementary material.

Acknowledgments

We thank J.F. Anderson (Connecticut Agricultural Experiment Station) for WNV, and J.U. Jung (University of Southern California) for plasmids. Supported by the National Institutes of Health (AI-055749 and AI-50031), the Howard Hughes Medical Institute (E.F.), the Northeast Biodefense Center (U54-AI057158-Lipkin to P.W.) and the Canadian Institutes for Health Research (79410 to M.S.).

References

1. Lamkanfi M, Festjens N, Declercq W, Vanden Berghe T, Vandenabeele P. Caspases in cell survival, proliferation and differentiation. Cell Death Differ. 2007; 14:44–55. [PubMed: 17053807]
2. Scott AM, Saleh M. The inflammatory caspases: guardians against infections and sepsis. Cell Death Differ. 2007; 14:23–31. [PubMed: 16977333]
3. Saleh M, et al. Differential modulation of endotoxin responsiveness by human caspase-12 polymorphisms. Nature. 2004; 429:75–79. [PubMed: 15129283]
4. Saleh M, et al. Enhanced bacterial clearance and sepsis resistance in caspase-12-deficient mice. Nature. 2006; 440:1064–1068. [PubMed: 16625199]
5. Franchi L, Eigenbrod T, Munoz-Planillo R, Nunez G. The inflammasome: a caspase-1-activation platform that regulates immune responses disease pathogenesis. Nat. Immunol. 2009; 10:241–247. [PubMed: 19221555]
6. Ichinohe T, Lee HK, Ogura Y, Flavell R, Iwasaki A. Inflammasome recognition of influenza virus is essential for adaptive immune responses. J. Exp. Med. 2009; 206:79–87. [PubMed: 19139171]
7. Allen IC, et al. The NLRP3 inflammasome mediates in vivo innate immunity to influenza A virus through recognition of viral RNA. Immunity. 2009; 30:556–565. [PubMed: 19362020]
8. Thomas PG, et al. The intracellular sensor NLRP3 mediates key innate and healing responses to influenza A virus via the regulation of caspase-1. Immunity. 2009; 30:566–575. [PubMed: 19362023]
9. Poeck H, et al. Recognition of RNA virus by RIG-I results in activation of CARD9 and inflammasome signaling for interleukin 1β production. Nat. Immunol. 2009; 11:63–69. [PubMed: 19915568]
10. Roy S, et al. Confinement of caspase-12 proteolytic activity to autoprocessing. Proc. Natl. Acad. Sci. USA. 2008; 105:4133–4138. [PubMed: 18332441]
11. LeBlanc PM, et al. Caspase-12 modulates NOD signaling and regulates antimicrobial peptide production and mucosal immunity. Cell Host Microbe. 2008; 3:146–157. [PubMed: 18329614]
12. Nakagawa T, et al. Caspase-12 mediates endoplasmic-reticulum-specific apoptosis and cytotoxicity by amyloid-β. Nature. 2000; 403:98–103. [PubMed: 10638761]
13. Tan Y, et al. Ubiquitous calpains promote caspase-12 and JNK activation during endoplasmic reticulum stress-induced apoptosis. J. Biol. Chem. 2006; 281:16016–16024. [PubMed: 16597616]
14. Yoneda T, et al. Activation of caspase-12, an endoplastic reticulum (ER) resident caspase through tumor necrosis factor receptor-associated factor 2-dependent mechanism in response to the ER stress. J. Biol. Chem. 2001; 276:13935–13940. [PubMed: 11278723]

15. Rao RV, et al. Coupling endoplasmic reticulum stress to the cell death program. Mechanism of caspase activation. J. Biol. Chem. 2001; 276:33869–33874. [PubMed: 11448953]
16. Groenendyk J, Michalak M. Endoplasmic reticulum quality control and apoptosis. Acta Biochim. Pol. 2005; 52:381–395. [PubMed: 15933766]
17. Rao RV, et al. Coupling endoplasmic reticulum stress to the cell death program. An Apaf-1-independent intrinsic pathway. J. Biol. Chem. 2002; 277:21836–21842. [PubMed: 11919205]
18. Obeng EA, Boise LH. Caspase-12 caspase-4 are not required for caspase-dependent endoplasmic reticulum stress-induced apoptosis. J. Biol. Chem. 2005; 280:29578–29587. [PubMed: 15975932]
19. Di Sano F, et al. Endoplasmic reticulum stress induces apoptosis by an apoptosome-dependent but caspase 12-independent mechanism. J. Biol. Chem. 2006; 281:2693–2700. [PubMed: 16317003]
20. Martinon F, Tschopp J. Inflammatory caspases and inflammasomes: master switches of inflammation. Cell Death Differ. 2007; 14:10–22. [PubMed: 16977329]
21. Barton GM, Medzhitov R. Linking Toll-like receptors to IFN-α/β expression. Nat. Immunol. 2003; 4:432–433. [PubMed: 12719735]
22. Yoneyama M, et al. The RNA helicase RIG-I has an essential function in double-stranded RNA-induced innate antiviral responses. Nat. Immunol. 2004; 5:730–737. [PubMed: 15208624]
23. Yoneyama M, et al. Shared unique functions of the DExD/H-box helicases RIG-I, MDA5, and LGP2 in antiviral innate immunity. J. Immunol. 2005; 175:2851–2858. [PubMed: 16116171]
24. Wang T, et al. Toll-like receptor 3 mediates West Nile virus entry into the brain causing lethal encephalitis. Nat. Med. 2004; 10:1366–1373. [PubMed: 15558055]
25. Daffis S, Samuel MA, Suthar MS, Gale M Jr, Diamond MS. Toll-like receptor 3 has a protective role against West Nile virus infection. J. Virol. 2008; 82:10349–10358. [PubMed: 18715906]
26. Town T, et al. Toll-like receptor 7 mitigates lethal West Nile encephalitis via interleukin 23-dependent immune cell infiltration and homing. Immunity. 2009; 30:242–253. [PubMed: 19200759]
27. Fredericksen BL, Keller BC, Fornek J, Katze MG, Gale M Jr. Establishment and maintenance of the innate antiviral response to West Nile Virus involves both RIG-I and MDA5 signaling through IPS-1. J. Virol. 2008; 82:609–616. [PubMed: 17977974]
28. Loo YM, et al. Distinct RIG-I MDA5 signaling by RNA viruses in innate immunity. J. Virol. 2008; 82:335–345. [PubMed: 17942531]
29. Gack MU, et al. TRIM25 RING-finger E3 ubiquitin ligase is essential for RIG-I-mediated antiviral activity. Nature. 2007; 446:916–920. [PubMed: 17392790]
30. Arimoto K, et al. Negative regulation of the RIG-I signaling by the ubiquitin ligase RNF125. Proc. Natl. Acad. Sci. USA. 2007; 104:7500–7505. [PubMed: 17460044]
31. Jounai N, et al. The Atg5 Atg12 conjugate associates with innate antiviral immune responses. Proc. Natl. Acad Sci. USA. 2007; 104:14050–14055. [PubMed: 17709747]
32. Saito T, et al. Regulation of innate antiviral defenses through a shared repressor domain in RIG-I and LGP2. Proc. Natl. Acad. Sci. USA. 2007; 104:582–587. [PubMed: 17190814]
33. Satoh T, et al. LGP2 is a positive regulator of RIG-I- and MDA5-mediated antiviral responses. Proc. Natl. Acad. Sci. USA. 2010; 107:1512–1517. [PubMed: 20080593]
34. Simon D, et al. Friedreich ataxia mouse models with progressive cerebellar and sensory ataxia reveal autophagic neurodegeneration in dorsal root ganglia. J. Neurosci. 2004; 24:1987–1995. [PubMed: 14985441]
35. Kato H, et al. Differential roles of MDA5 and RIG-I helicases in the recognition of RNA viruses. Nature. 2006; 441:101–105. [PubMed: 16625202]
36. Yoneyama M, Fujita T. Function of RIG-I-like receptors in antiviral innate immunity. J. Biol. Chem. 2007; 282:15315–15318. [PubMed: 17395582]
37. Fabian Z, Csatary CM, Szeberenyi J, Csatary LK. p53-independent endoplasmic reticulum stress-mediated cytotoxicity of a Newcastle disease virus strain in tumor cell lines. J. Virol. 2007; 81:2817–2830. [PubMed: 17215292]
38. Li XD, Lankinen H, Putkuri N, Vapalahti O, Vaheri A. Tula hantavirus triggers pro-apoptotic signals of ER stress in Vero E6 cells. Virology. 2005; 333:180–189. [PubMed: 15708603]

39. Jordan R, Wang L, Graczyk TM, Block TM, Romano PR. Replication of a cytopathic strain of bovine viral diarrhea virus activates PERK and induces endoplasmic reticulum stress-mediated apoptosis of MDBK cells. J. Virol. 2002; 76:9588–9599. [PubMed: 12208938]
40. Bitko V, Barik S. An endoplasmic reticulum-specific stress-activated caspase(caspase-12) is implicated in the apoptosis of A549 epithelial cells by respiratory syncytial virus. J. Cell. Biochem. 2001; 80:441–454. [PubMed: 11135374]
41. Samuel MA, Morrey JD, Diamond MS. Caspase 3-dependent cell death of neurons contributes to the pathogenesis of West Nile virus encephalitis. J. Virol. 2007; 81:2614–2623. [PubMed: 17192305]
42. Shrestha B, Gottlieb D, Diamond MS. Infection and injury of neurons by West Nile encephalitis virus. J. Virol. 2003; 77:13203–13213. [PubMed: 14645577]
43. Sejvar JJ, et al. Neurocognitive and functional outcomes in persons recovering from West Nile virus illness. J. Neuropsychol. 2008; 2:477–499. [PubMed: 19824176]
44. Kobayashi K, et al. RICK/Rip2/CARDIAK mediates signalling for receptors of the innate and adaptive immune systems. Nature. 2002; 416:194–199. [PubMed: 11894098]
45. Takahashi K, et al. Roles of caspase-8 and caspase-10 in innate immune responses to double-stranded RNA. J. Immunol. 2006; 176:4520–4524. [PubMed: 16585540]
46. Kim MJ, Yoo JY. Active caspase-1-mediated secretion of retinoic acid inducible gene-I. J. Immunol. 2008; 181:7324–7331. [PubMed: 18981155]
47. Tian Z, Shen X, Feng H, Gao B. IL-1 beta attenuates IFN-αβ-induced antiviral activity and STAT1 activation in the liver: involvement of proteasome-dependent pathway. J. Immunol. 2000; 165:3959–3965. [PubMed: 11034404]
48. Yeretssian G, et al. Gender differences in expression of the human caspase-12 long variant determines susceptibility to *Listeria monocytogenes* infection. Proc. Natl. Acad Sci. USA. 2009; 106:9016–9020. [PubMed: 19447924]
49. Escribese MM, et al. Estrogen inhibits dendritic cell maturation to RNA viruses. Blood. 2008; 112:4574–4584. [PubMed: 18802009]
50. Clark HB, et al. Purkinje cell expression of a mutant allele of SCA1 in transgenic mice leads to disparate effects on motor behaviors, followed by a progressive cerebellar dysfunction and histological alterations. J. Neurosci. 1997; 17:7385–7395. [PubMed: 9295384]

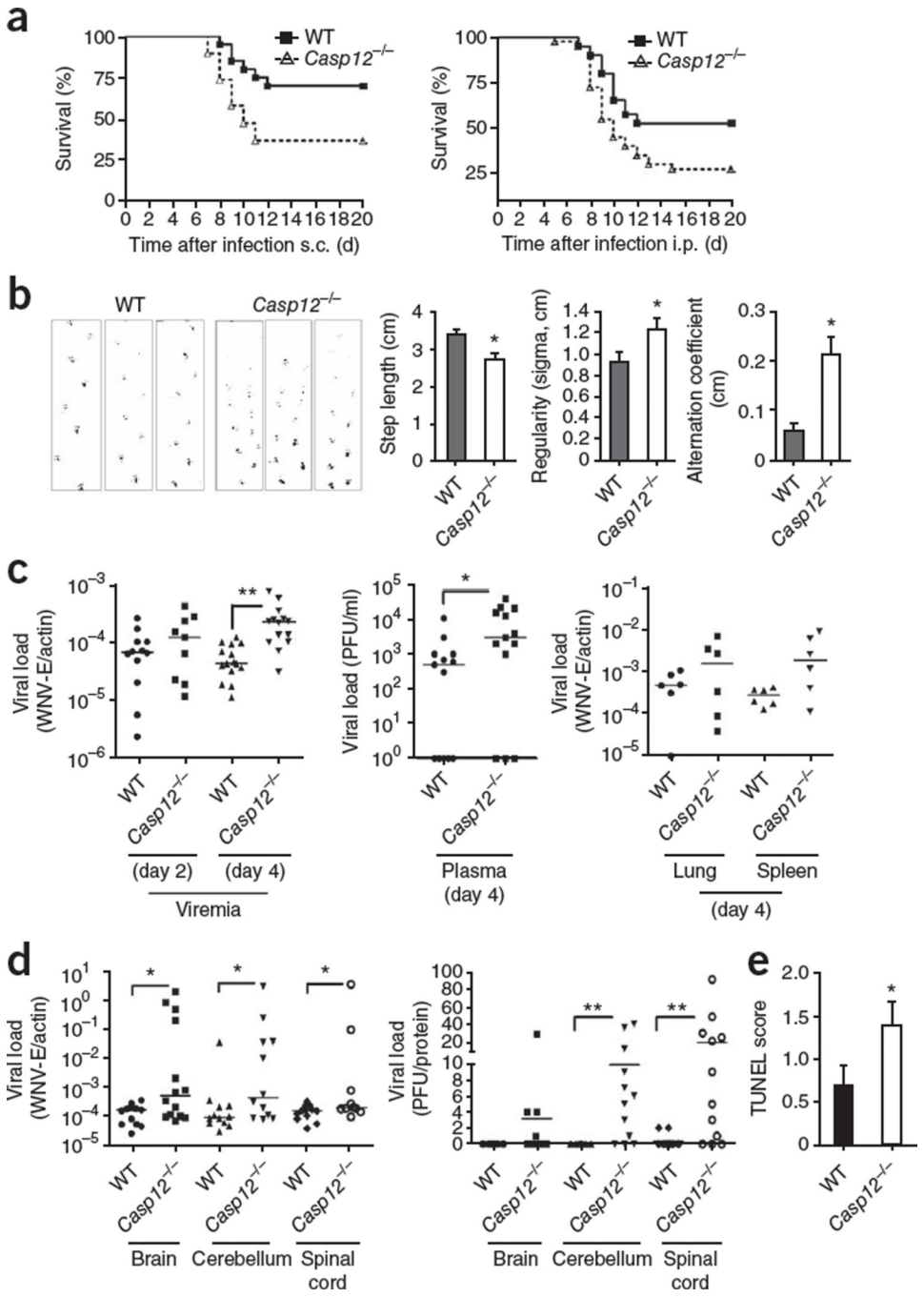

Figure 1.

Casp12$^{-/-}$ mice are more prone to WNV encephalitis and develop exacerbated neurological symptoms. (**a**) Mortality of age- and sex-matched wild-type (WT; C57BL/6) and *Casp12*$^{-/-}$ mice inoculated subcutaneously (s.c.; $n = 20$ mice per group) or intraperitoneally (i.p.; $n = 40$ mice per group) with 200 or 1,500 PFU of WNV and monitored daily for 20 d. $P = 0.024$ (subcutaneous) or 0.017 (intraperitoneal). Data were pooled from three independent experiments. (**b**) Footprint analysis on day 5 after infection (intraperitoneal injection): step length, average distance of forward movement between alternate steps; regularity, assessed as sigma, the standard variation of all right-right and left-left step distances; and alternation

coefficient (uniformity), mean of the ratio of right-left step distance to right-right step distance. *$P < 0.05$ (two-tailed Student's *t*-test). Data are representative of two experiments (mean and s.e.m.; $n = 5$ mice per group). (c,d) Viral load in the periphery (**c**) or CNS (**d**) of mice at day 8 after subcutaneous infection with 200 PFU of WNV, assessed by quantitative PCR analysis of WNV-E (presented relative to mouse β-actin) or plaque assay (presented as PFU per 30 μg total protein). Each symbol represents one mouse; small horizontal lines indicate the mean. *$P < 0.05$ and **$P < 0.01$ (nonparametric Mann-Whitney analysis). Data are representative of two experiments. (**e**) TUNEL assay of CNS apoptosis on day 8 after infection as in **c,d**. *$P < 0.05$ (Student's *t*-test) Data are representative of two experiments (mean and s.e.m.; $n = 10$ mice per group)

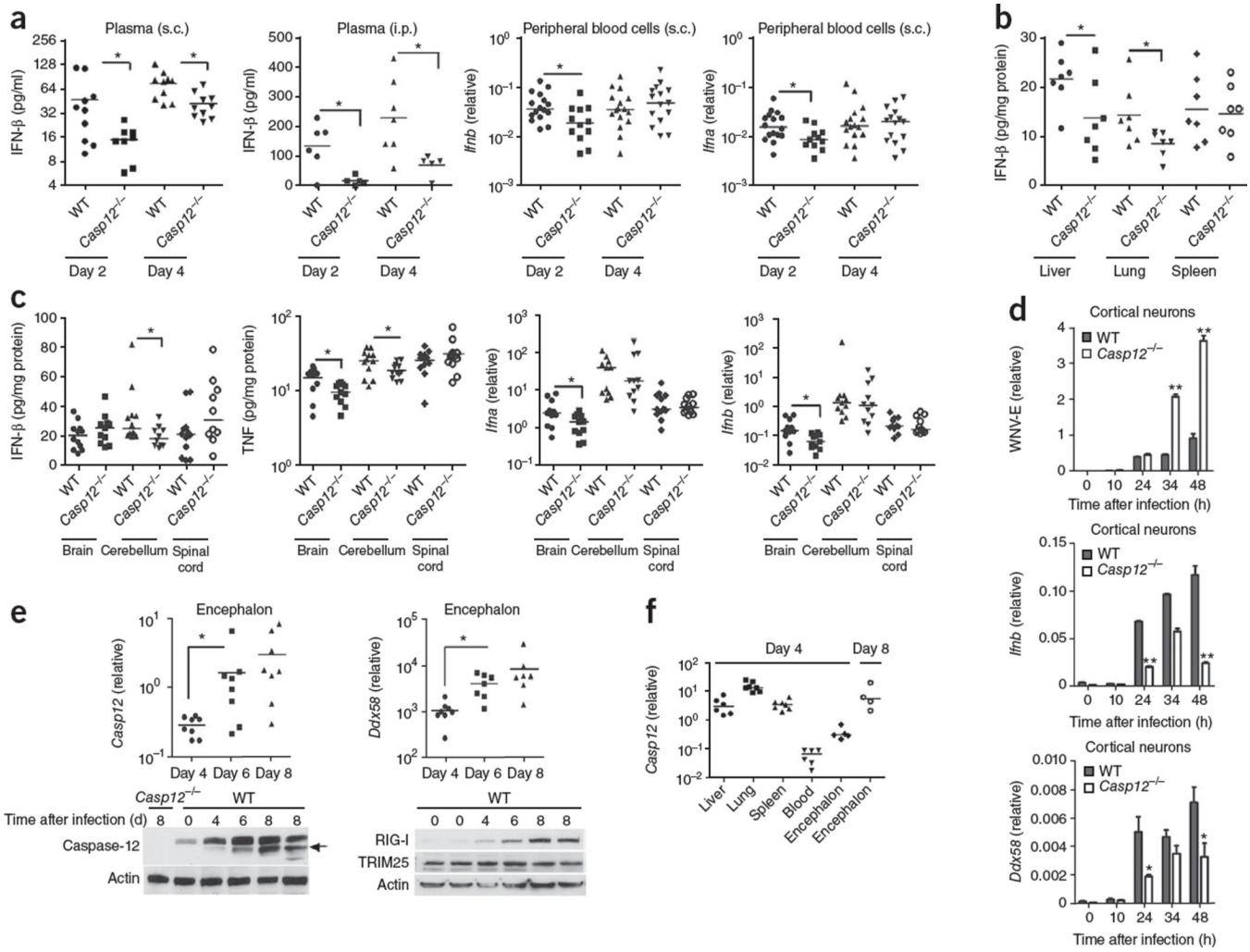

Figure 2.

Caspase-12 is required for an effective type I interferon response to WNV *in vivo* and *in vitro*. (**a**) Enzyme-linked immunosorbent assay (ELISA) or quantitative PCR analysis of the plasma concentration of IFN-β and transcript abundance of *Ifnb* and *Ifna* (relative to β-actin expression) in blood cells from mice at days 2 and 4 after infection with 200 PFU of WNV subcutaneously or 1,500 PFU of WNV intraperitoneally. (**b**) ELISA of IFN-β in peripheral tissues at day 4 after subcutaneous infection with 200 PFU of WNV. (**c**) ELISA of IFN-β and TNF and quantitative PCR analysis of *Ifnb* and *Ifna* (relative to β-actin expression) in the CNS at day 8 after subcutaneous infection with 200 PFU of WNV. (**d**) Quantitative PCR analysis of transcripts for WNV-E, IFN-β (*Ifnb*) and RIG-I (*Ddx58*) in primary cortical neurons infected with WNV at a multiplicity of infection (MOI) of 1; results are presented relative to those of β-actin. (**e**) Quantitative PCR (top) and immunoblot analysis (below) of caspase-12 and RIG-I transcripts (top; normalized to β-actin) and protein (below) in the encephalon. Arrow indicates the cleaved products of caspase-12. (**f**) *Casp12* mRNA in various tissues after subcutaneous WNV challenge. In **a**–**c**,**e**,**f**, each dot represents one mouse; small horizontal lines indicate the mean. $*P < 0.05$ and $**P < 0.01$ (nonparametric Mann-Whitney test or Student's *t*-test). Data are representative of two experiments (mean and s.e.m. in **d**).

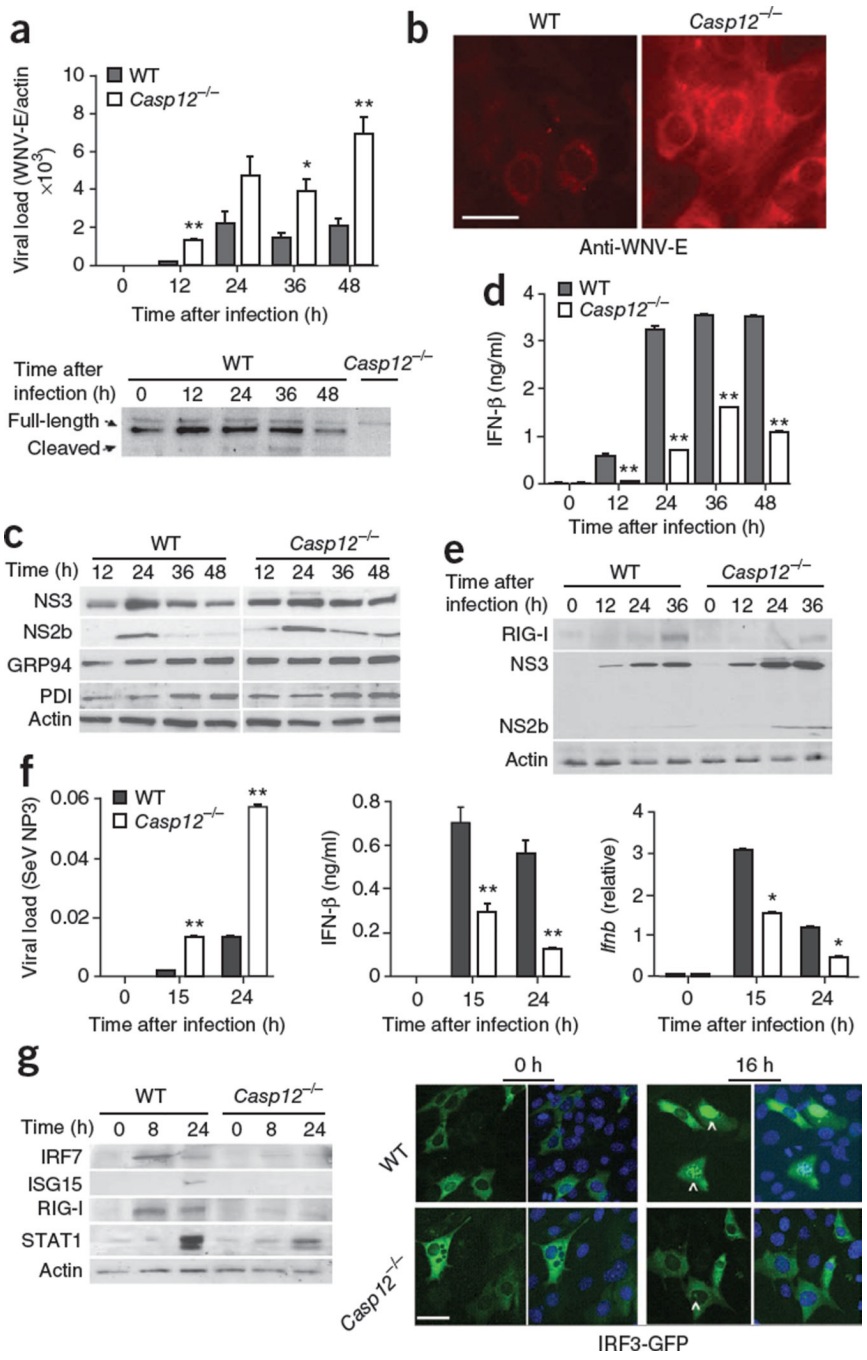

Figure 3.

Caspase-12 is important for the type I interferon response to WNV and SeV in MEFs. (**a**) Viral loads in MEFs infected for 0–48 h with WNV (MOI, 1), assessed by quantitative PCR analysis of WNV-E and presented relative to mouse β-actin (top), and immunoblot analysis of caspase-12 in those MEFs (below). Arrows indicate caspase-12 protein. (**b**) Fluorescence microscopy of WNV in MEFs at 24 h after infection (MOI, 1), visualized with antibody to WNV-E (anti-WNV-E) conjugated to the rhodamine dye TRITC. Scale bar, 20 μm. (**c**) Immunoblot analysis of NS3, NS2b, GRP94 and PDI in MEFs infected for 12–48 h with WNV (MOI, 1). (**d**) ELISA of IFN-β in the cell culture medium of MEFs infected for 0–48

h with WNV (MOI, 1). (**e**) Immunoblot analysis of RIG-I, NS3 and NS2b in MEFs infected for 0–36 h with WNV (MOI, 1). (**f**) Viral load in MEFs infected with SeV (MOI, 1), assessed by quantitative PCR analysis of SeV NP3 and presented relative to mouse β-actin (left), and ELISA of IFN-β protein in the cell culture medium and quantitative PCR analysis of *Ifnb* transcripts (relative to β-actin) of MEFs infected with SeV (MOI, 1). (**g**) Immunoblot analysis (left) of the ISG proteins IRF7, ISG15, RIG-I and STAT1 in MEFs infected for 0, 8 or 24 h with SeV (MOI, 1), and microscopy of nuclear localization (arrowheads) of GFP-tagged interferon-regulatory factor 3 (IRF3-GFP) in those cells. Scale bar, 20 μm. $*P < 0.05$ and $**P < 0.01$ (two-tailed Student's *t*-test). Data are representative of three independent experiments (mean and s.e.m. in **a,d,f**).

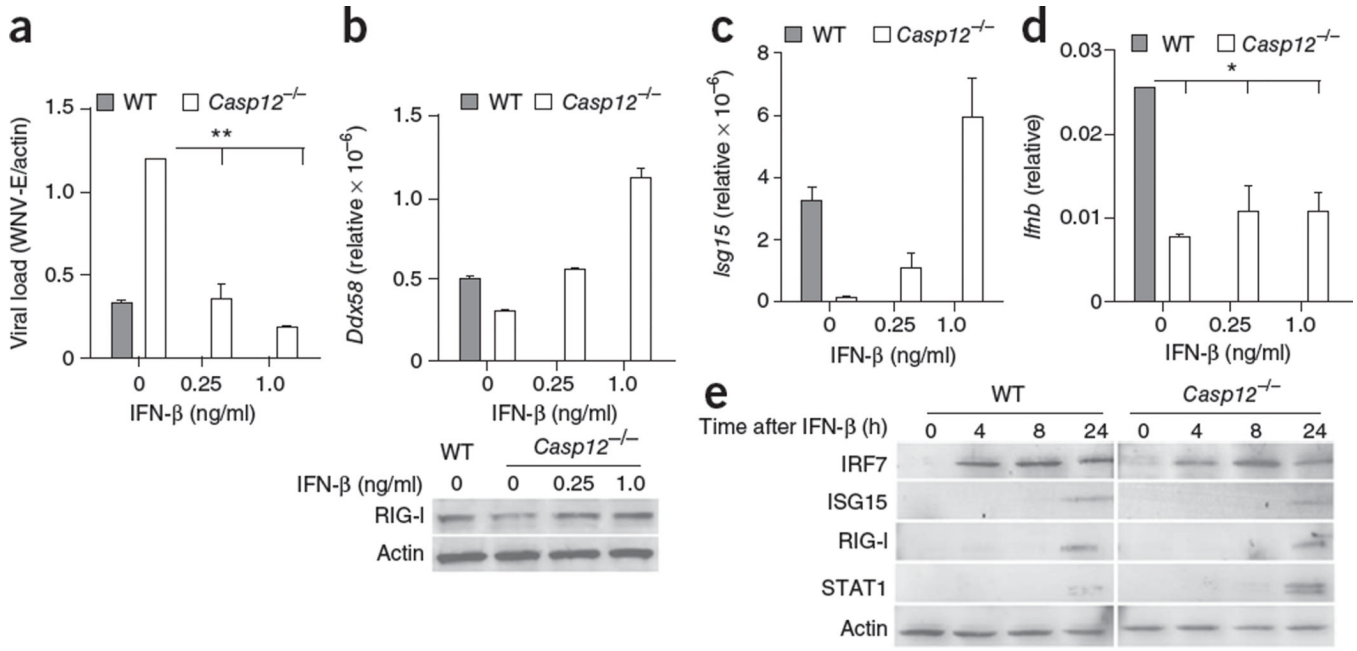

Figure 4.

IFN-α and IFN-βS signaling is intact in *Casp12*$^{-/-}$ MEFs. (**a**) Viral load in MEFs treated for 1 h with recombinant mouse IFN-(3, followed by infection for 24 h with WNV (MOI, 1), assessed by quantitative PCR analysis of WNV-E and presented relative to mouse β-actin. (**b**) Quantitative PCR and immunoblot analysis of RIG-I mRNA (*Ddx58*; presented relative to β-actin) and RIG-I protein, respectively, in MEFs treated as in a. (**c**) Quantitative PCR analysis of *Isg15* transcripts (**c**) and endogenous *Ifnb* transcripts (**d**) in MEFs treated as in a; results are presented relative to (3-actin. (e) Immunoblot analysis of IRF7, ISG15, RIG-I and STAT1 in MEFs treated with recombinant mouse IFN- βalone (1 ng/ml). *$P < 0.05$ and **$P < 0.01$ (two-tailed Student's *t*-test). Data are representative of three independent experiments (mean and s.e.m. in **a**–**d**).

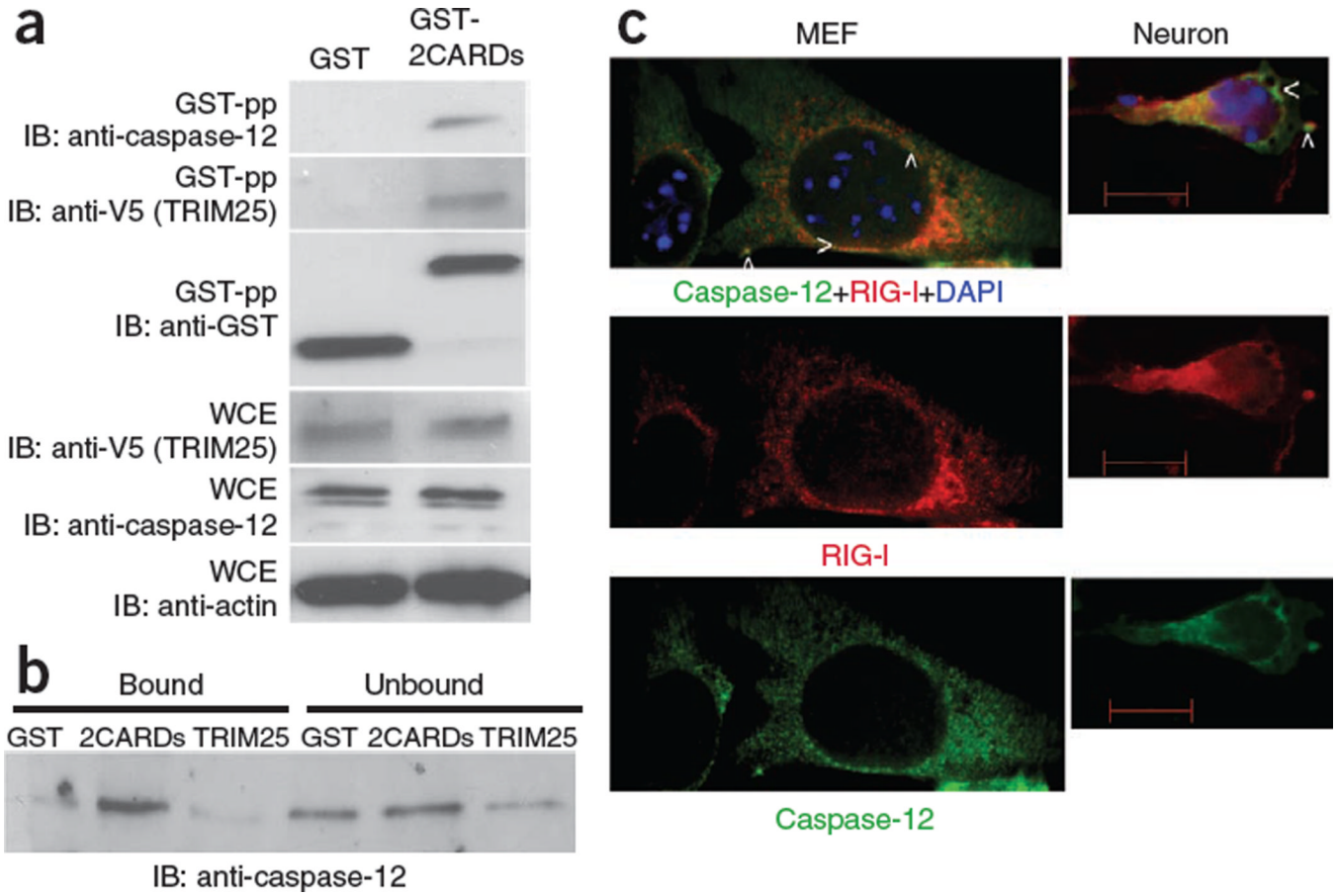

Figure 5.

Caspase-12 interacts with RIG-I. (**a**) Immunoblot analysis (IB) of GST-precipitated (GST-pp) proteins from MEFs transfected with plasmid alone (GST) or plasmid encoding the two CARDs conjugated to GST (GST-2CARDs), together with plasmid encoding caspase-12 and V5-tagged TRIM25. WCE, whole-cell extract (no precipitation). (**b**) Binding of GST or GST-2CARDs (affinity purified from *E. coli*) or TRIM25 to purified caspase-12 (cleaved from GST-tagged caspase-12) or TRIM25. (**c**) Microscopy of MEFs or primary cortical neurons cotransfected with plasmids expressing GFP-labeled caspase-12 and RIG-I and infected for 12 h with WNV (MOI, 5); RIG-I was stained with anti-RIG-I and TRITC-conjugated secondary antibody. Arrows indicate some colocalization. DAPI, DNA-intercalating dye. Scale bar, 10 μm. Data are representative of two experiments.

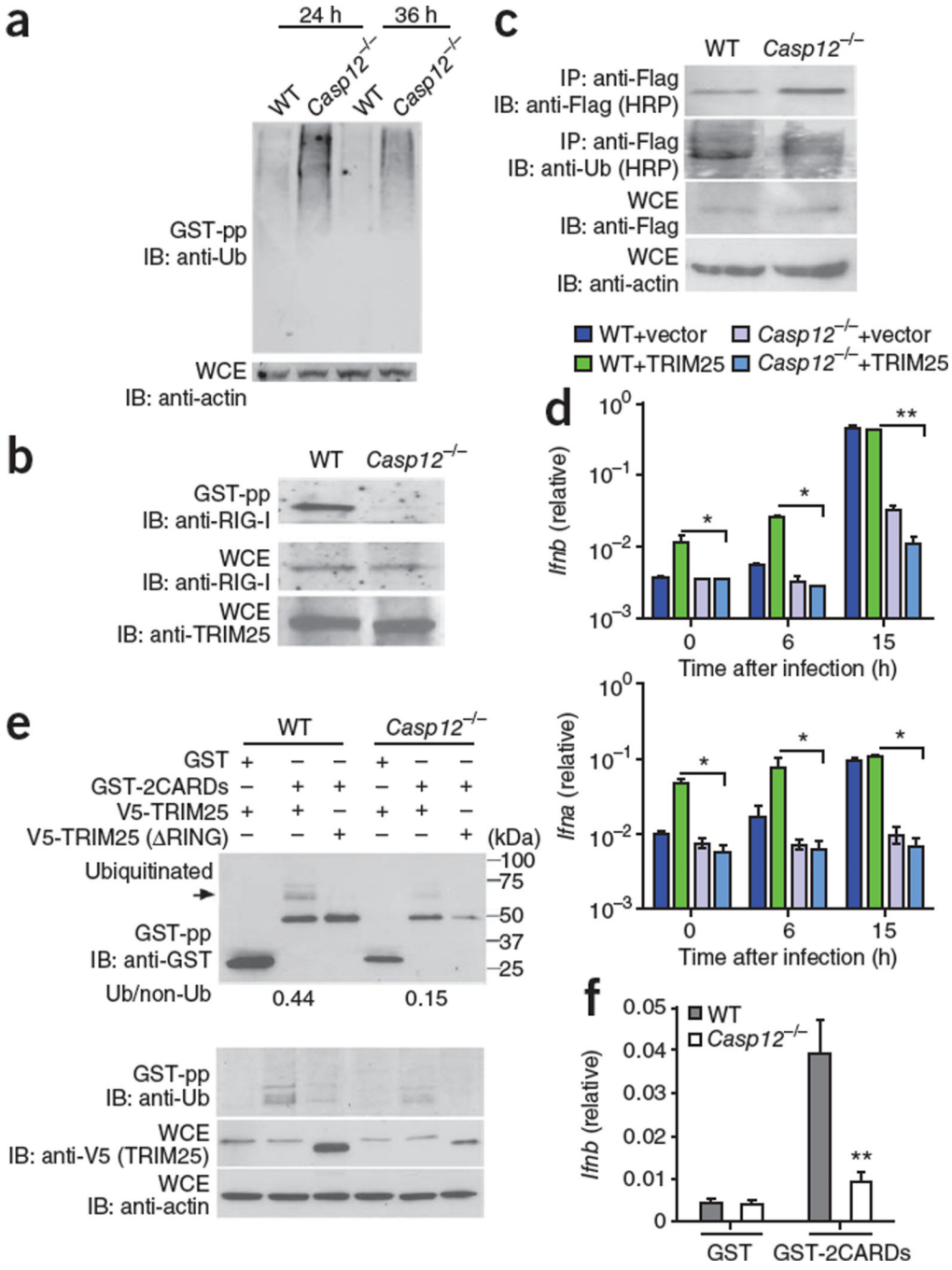

Figure 6.

Caspase-12 regulates RIG-I ubiquitination. (**a**) Immunoblot analysis of total polyubiquitinated proteins in MEFs transfected with RIG-I-expressing plasmid and infected for 24 h with WNV, followed by purification of polyubiquitinated proteins with a GST module; proteins were detected with horseradish peroxidase (HRP)–conjugated anti-ubiquitin (anti-Ub). (**b**) Immunoblot analysis of ubiquitinated RIG-I (GST-pp) and total RIG-I or TRIM25 (WCE) in MEFs treated as in **a**; proteins were detected with anti-RIG-I or anti-TRIM25. (**c**) Immunoblot analysis of RIG-I immunoprecipitated with anti-Flag from MEFs transfected with Flag-tagged RIG-I plasmid and infected for 24 h with WNV. (**d**).

Quantitative PCR analysis of *Ifnb* and *Ifna* transcripts in MEFs transfected with RIG-I plasmid together with vector-only or V5-tagged TRIM25 plasmid, followed by infection for 0, 6 or 15 h with WNV; results are presented relative to mouse β-actin. (**e**) Immunoblot analysis of GST-precipitated proteins from wild-type or *Casp12*$^{-/-}$ MEFs transfected for 20 h with various combinations of plasmid alone (GST) and/or plasmid encoding the two CARDs (GST-2CARDs), V5-tagged TRIM25 (V5-TRIM25) or V5-tagged TRIM25 lacking the RING (V5-TRIM25 (ΔRING)). Right margin, molecular size (in kilodaltons (kDa)). (**f**) Quantitative PCR analysis of *Ifnb* in MEFs transfected for 20 h with plasmid alone (GST) or plasmid encoding the two CARDs (GST-2CARDs). *$P < 0.01$ (two-tailed Student's *t*-test). Data are representative of two (**a,c**–**f**) or three (**b**) experiments (mean and s.e.m. in **d**).